⌘ *Author's Choice*

Epidermal Growth Factor Receptor Phosphorylation Sites Ser[991] and Tyr[998] Are Implicated in the Regulation of Receptor Endocytosis and Phosphorylations at Ser[1039] and Thr[1041]*[S]

Jiefei Tong‡, Paul Taylor‡, Scott M. Peterman§, Amol Prakash§, and Michael F. Moran‡¶‖

Aberrant expression, activation, and down-regulation of the epidermal growth factor receptor (EGFR) have causal roles in many human cancers, and post-translational modifications including phosphorylation and ubiquitination and protein-protein interactions directly modulate EGFR function. Quantitative mass spectrometric analyses including selected reaction monitoring (also known as multiple reaction monitoring) were applied to the EGFR and associated proteins. In response to epidermal growth factor (EGF) stimulation of cells, phosphorylations at EGFR Ser[991] and Tyr[998] accumulated more slowly than at receptor sites involved in RAS-ERK signaling. Phosphorylation-deficient mutant receptors S991A and Y998F activated ERK in response to EGF but were impaired for receptor endocytosis. Consistent with these results, the mutant receptors retained a network of interactions with known signaling proteins including EGF-stimulated binding to the adaptor GRB2. Compared with wild type EGFR the Y998F variant had diminished EGF-stimulated interaction with the ubiquitin E3 ligase CBL, and the S991A variant had decreased associated ubiquitin. The endocytosis-defective mutant receptors were found to have elevated phosphorylation at positions Ser[1039] and Thr[1041]. These residues reside in a serine/threonine-rich region of the receptor previously implicated in p38 mitogen-activated protein kinase-dependent stress/cytokine-induced EGFR internalization and recycling (Zwang, Y., and Yarden, Y. (2006) p38 MAP kinase mediates stress-induced internalization of EGFR: implications for cancer chemotherapy. *EMBO J.* 25, 4195–4206). EGF-induced phosphorylations at Ser[1039] and Thr[1041] were blocked by treatment of cells with SB-202190, a selective inhibitor of p38. These results suggest that coordinated phosphorylation of EGFR involving sites Tyr[998], Ser[991], Ser[1039], and Thr[1041] governs the trafficking of EGF receptors. This reinforces the notion that EGFR function is manifest through spatially and temporally controlled protein-protein interactions and phosphorylations. *Molecular & Cellular Proteomics 8: 2131–2144, 2009.*

Upon activation by ligand, the epidermal growth factor receptor (EGFR)[1] dimerizes, sometimes as heterodimers with other EGFR family members; is catalytically activated by reorientation of kinase region subdomains; becomes covalently modified by phosphorylation and ubiquitination; and interacts with a variety of intracellular proteins (1, 2). These events activate intracellular signaling cascades, and concurrently the dimerized receptors become internalized through endocytosis and then may be recycled to the cell surface or degraded in lysosomes (3). Systematic analysis of EGFR family phosphorylation-dependent protein interactions has been assessed (4, 5), and many of the known EGFR-interacting proteins can be categorized as functioning in cellular processes such as EGF-induced signal transduction and EGFR endocytosis and trafficking. Temporal analysis of tyrosine phosphorylation following EGF treatment of cells revealed groups of EGFR substrates with shared profiles of phosphorylation kinetics, including some that display rapid kinetics of phosphorylation accumulation and are involved in signal trans-

From the ‡Program in Molecular Structure and Function, The Hospital For Sick Children, and The McLaughlin Centre For Molecular Medicine and ¶Department of Molecular Genetics and Banting and Best Department of Medical Research, University of Toronto, Toronto, Ontario M5G 1L7, Canada and §ThermoFisher Biomarker Research Initiatives in Mass Spectrometry Center, Cambridge, Massachusetts 02139

⌘ *Author's Choice*—Final version full access.

Received, March 18, 2009, and in revised form, May 19, 2009

Published, MCP Papers in Press, June 15, 2009, DOI 10.1074/mcp.M900148-MCP200

[1] The abbreviations used are: EGFR, epidermal growth factor receptor; EGF, epidermal growth factor; ERK, extracellular signal-regulated kinase; SRM, selected reaction monitoring; MAP, mitogen-activated protein; TNF, tumor necrosis factor; E3, ubiquitin-protein isopeptide ligase; GFP, green fluorescent protein; IP, immunoprecipitation; HEK293, human embryonic kidney 293; NHS, *N*-hydroxysuccinimide; TSQ, triple stage quadrupole; CV, coefficient of variation; WT, wild type; IPI, International Protein Index.

duction (*e.g.* ERK kinase activation) and others that accumulate more slowly following ligand treatment and are involved in receptor internalization and down-regulation (5–11). Although advances in MS and the definition of phosphorylation-dependent protein-protein interactions have led to a greatly expanded view of EGFR function and regulation, our understanding of the biological consequences and spatial-temporal relationships of individual modifications is incomplete.

In a previous quantitative phosphoproteomics study aimed at the identification of drug-modulated changes in phosphorylation associated with the EGFR network, a cluster of three sites of phosphorylation in the EGFR carboxyl tail region was identified as affected by receptor stimulation by EGF and inhibited by the ATP-competitive EGFR inhibitor PKI166 in human A431 tumor cells and xenograft tumors (12). The three sites in the cluster, Ser^{991},[2] Ser^{995}, and Tyr^{998}, are localized within a single tryptic peptide having the sequence MHLPSPTDSNFYR that spans residues 987–999. The phosphorylation of Tyr^{998} was first described by Stover *et al.* (12), whereas the two serine sites were shown previously to be phosphorylated by Heisermann and Gill (13). Numerous recent studies using different cultured cell models have verified the phosphorylation of EGFR at Tyr^{998} and Ser^{991} (10, 11, 14, 15), and Thr^{993} was also observed to be phosphorylated within this same region of the EGFR in EGF-stimulated HeLa cells (10). The modulation of these sites by EGF and the EGFR inhibitor implicates them in EGFR signaling and suggests that they may have utility as pharmacodynamic markers of EGFR activity. However, the function and importance of these sites, their modulation by kinases and phosphatases, and possible roles in EGFR function remain unknown.

Several amino acid residues in the EGFR have been implicated in the regulation of its trafficking. Sorkin *et al.* (16) showed that substitution of Tyr^{998} with phenylalanine rendered high density EGFRs defective for endocytosis and interaction with AP-2. More recent kinetic studies using MS indicated that EGFR phosphorylation at both Tyr^{998} (5) and Ser^{991} (10) occurs relatively slowly compared with other EGF-induced tyrosine phosphorylations known to be involved in receptor-proximal signal transduction. For example, Mann and co-workers (10) recorded maximal phosphorylation at EGFR sites Tyr^{1110}, Tyr^{1172}, and Tyr^{1197} at 1 min post-EGF, whereas EGF-stimulated phosphorylation at Tyr^{998} was still increasing at 15 min post-EGF (5), and a peptide containing both $Ser(P)^{991}$ and $Thr(P)^{993}$ peaked after 10 min (10). However, the role of phosphorylation at Tyr^{998} and Ser^{991} has not been reported. Another region of the EGFR, spanning residues 1026–1046, was identified by Zwang and Yarden (17) as a target of phosphorylation downstream of the stress-activated mitogen-activated protein (MAP) kinase p38 and associated with transient internalization and recycling of the EGFR in response to cytokine (TNFα) and stress challenges such as UV irradiation and the chemotherapeutic agent cisplatinum. Within this part of the receptor, a 13-residue section spanning 1029–1041 and the leucines at 1034 and 1035 in particular were found to be essential for ligand- and dimerization-induced EGFR endocytosis (18). Although both EGF- and stress-induced EGFR internalization may be clathrin-mediated, they differ in that the former leads to receptor down-regulation and involves the E3 ubiquitin ligase CBL (19), whereas the latter involves receptor recycling, is not associated with receptor phosphorylation at the CBL binding site $Tyr(P)^{1069}$, and, in the case of TNFα treatment, involves activation of the transforming growth factor β-activated kinase TAK1 upstream of p38 (20). Interestingly although p38 kinase is not required for EGF-induced EGFR internalization, it is required for CBL-dependent receptor degradation (21). Therefore, alternate pathways involving p38 kinase regulate the down-regulation or recycling of the EGFR in response to diverse extracellular signals. However, the molecular details that govern these two processes are not fully understood.

In the current study, EGFR phosphorylation, signaling, protein-protein interactions, and trafficking were analyzed to address the role of Tyr^{998} and Ser^{991} in EGFR endocytosis. This was achieved by application of complementary methods including quantitative selected reaction monitoring (SRM, also known as MRM for multiple reaction monitoring) mass spectrometry, fluorescence imaging and cell sorting, immunoaffinity protein enrichment and blotting, and site-directed mutagenesis. Substitution mutations that prevented phosphorylation at EGFR Tyr^{998} and Ser^{991} did not prevent EGFR-to-ERK signaling but impaired EGF-induced receptor internalization and stimulated p38 kinase-dependent receptor phosphorylation at positions Ser^{1039} and Thr^{1041}. These findings confirm the importance of Tyr^{998} and reveal a role for Ser^{991} in EGF-mediated EGFR internalization possibly involving cross-talk with the p38 kinase-dependent EGFR recycling pathway.

EXPERIMENTAL PROCEDURES

Constructs and Reagents—Site-directed mutagenesis was used to generate Tyr^{998}-to-Phe and Ser^{991}-to-Ala mutations in a construct encoding a chimeric EGFR-FLAG-GFP protein (22). For immunoprecipitation (IP) anti-FLAG-M2 was obtained from Sigma-Aldrich. For Western blotting, anti-FLAG and anti-Tyr(P) (4G10) were obtained from Sigma-Aldrich and Millipore (Billerica, MA), respectively. All other antibodies were obtained from Cell Signaling Technology (Danvers, MA). Toptips (200 μl) for preparing custom-made C_{18} tips were purchased from Canadian Life Science (Peterborough, Ontario, Canada). SB-202190 was from Sigma-Aldrich; all other chemical reagents were purchased from Sigma-Aldrich, and aqueous solutions were prepared using Milli-Q grade water (Millipore, Bedford, MA).

Cell Culture and Cell Lysis—Human embryonic kidney 293 (HEK293) cells and lines derived from them were maintained in Dulbecco's modified Eagle's medium supplemented with 10% bovine serum. HEK-EGFR was derived from HEK293 and stably expresses chimeric EGFR as described previously (22). HEK293 derivatives stably expressing chimeric EGFR Y998F and S991A variants were

[2] The convention for EGFR numbering includes the 24-residue signal sequence.

derived by similar methods (22), and all EGFR-expressing transfectants were cultured as described above and including G418 (400 μg/ml). For IP and Western blotting, cells were deprived of serum overnight, treated with or without EGF (10 min, 100 ng/ml, 37 °C), then rinsed with ice-cold PBS, and lysed in Nonidet P-40 buffer (50 mM Tris-HCl, pH 7.5, 150 mM sodium chloride, 1% (v/v) Nonidet P-40, 100 mM NaF, 1 mM sodium orthovanadate, and protease inhibitors). In advance of MS analysis, prior to immunoprecipitation cell lysates were further clarified by ultracentrifugation for 60 min at 100,000 × *g*. For inhibition of p38 kinase, SB-202190 was used at a final concentration of 50 μM, a concentration at which it is not expected to affect ERK1/2, c-Jun NH_2-terminal kinase (JNK), and several other related kinases (23).

Fluorescence Microscopy and Flow Cytometry—For fluorescence imaging cells were cultured to subconfluence, deprived of serum overnight, and then treated with or without EGF (100 ng/ml) for 60 min at 4 °C and then at 37 °C for 0, 5, or 15 min. Cells were then fixed (3.7% paraformaldehyde, 23 °C, 10 min), washed with PBS, and observed by fluorescence microscopy as described previously (24).

For biotin labeling EGFR on the cell surface, cells were grown in 60-mm dishes to subconfluence, deprived of serum overnight, and then treated with or without EGF (50 ng/ml, 37 °C, 30 min). Biotinylation of intact cells was carried out as described by Zhang *et al.* (25). Briefly cells were suspended to 2.5 × 10^7 cells/ml in PBS (pH 8.0) and then incubated with 1.0 mg/ml sulfo-NHS-biotin (Pierce) at 23 °C for 30 min. Cells were then washed three times with PBS, lysed, and subjected to IP with immobilized anti-FLAG. Western blotting was performed as described below. The biotin detection agent was streptavidin-horseradish peroxidase.

For flow cytometry, cells at 80% confluence were deprived of serum overnight and then incubated with rhodamine-EGF at 4 °C for 30 min. After washing, cells were incubated at 37 °C for various time points (see Fig. 4*B*). After an acidic wash (0.2 M acetic acid and 0.5 M NaCl, pH 2.8) to remove non-internalized EGF, the fluorescence emission of internalized EGF was detected by flow cytometry (26).

IP and Western Blotting—For IP-Western analysis of associated proteins, 2 mg of total cellular protein in clarified lysates were extracted with immobilized anti-FLAG beads (10 μl) overnight at 4 °C. Immunoprecipitates were washed three times with Nonidet P-40 buffer, and proteins were eluted with 30 μl of 2× Laemmli sample buffer. Following SDS-PAGE proteins were electrophoretically transferred to Immobilon-P membranes (Millipore), then developed by using chemiluminescence reagents, imaged with x-ray film (Eastman Kodak Co. XRP), and quantified by using a Fluor-S MultiImager (Bio-Rad). For direct Western blotting of lysates, 40 μg protein were loaded per lane.

For MS analysis of IP samples, 5-fold more starting material (by protein amount) and 30 μl of anti-FLAG beads were used. Immunoprecipitates were washed three times with Nonidet P-40 buffer and twice with HPLC water and then eluted with 50 μl of 0.15% TFA. Proteins were further processed as described previously (22) and then analyzed as described below.

Mass Spectrometry—Samples were analyzed on a linear ion trap-Orbitrap hybrid analyzer (LTQ-Orbitrap, ThermoFisher, San Jose, CA) outfitted with a nanospray source and EASY-nLC split-free nano-LC system (Proxeon Biosystems, Odense, Denmark). The instrument method consisted of one MS full scan (400–1400 *m/z*) in the Orbitrap mass analyzer, an automatic gain control target of 500,000 with a maximum ion injection of 500 ms, one microscan, and a resolution of 60,000. Three data-dependent MS/MS scans were performed in the linear ion trap using the three most intense ions at 35% normalized collision energy. The MS and MS/MS scans were obtained in parallel fashion. In MS/MS mode automatic gain control targets were 10,000 with a maximum ion injection time of 100 ms. A minimum ion intensity of 1000 was required to trigger an MS/MS spectrum. The dynamic exclusion was applied using a maximum exclusion list of 500 with one repeat count with a repeat duration of 30 s and exclusion duration of 45 s.

SRM analysis was carried out by using a TSQ Quantum Ultra triple quadrupole MS instrument (Thermo Scientific) with a Proxeon source and LC system as described above except that the gradient time associated with the Orbitrap was 120 min and was 40 min with the TSQ instrument. Peptides were captured in a homemade 4-cm × 150-μm-inner diameter trapping column and eluted over a 20-cm × 75-μm-inner diameter fused silica analytical column. The packing material for both columns was Magic C_{18} (Michrom BioResources, Auburn, CA). The gradient was 0–65% acetonitrile in 0.1% formic acid over 35 min at 250 nl/min. The validated transitions for all phosphopeptides and unphosphorylated peptides for EGFR immunoprecipitates are listed in supplemental Table 1 and were monitored for the duration of the run. Most peptides were followed by using two unique transitions. Q2 gas pressure was 1.5 millitorrs, and collision energy was calculated relative to the precursor ion mass by the following formula: $m/z \times 0.034\ V + 3\ V$. The scan width was 0.02 Da, and the dwell time was 10 ms. Q1 was operated at a resolution of 0.2, and Q3 resolution was 0.7. Xcalibur data acquisition software and SRM Builder software (Thermo Scientific) were used for data acquisition and total ion current calculations.

MS Data Analysis—Tandem mass spectra were extracted by BioWorks version 3.3. All MS/MS samples were analyzed using SEQUEST (ThermoFinnigan, San Jose, CA; version 27, revision 12) and X! Tandem (The Global Proteome Machine Organization; version 2006.04.01.2). Both search engines were set up to search the IPI human database (version 3.18, 60,090 entries) assuming trypsin digestion, allowing two missed cleavages, and using a fragment ion mass tolerance of 0.5 Da and a parent ion tolerance of 0.02 Da. The iodoacetamide derivative of cysteine was specified as a fixed modification. The phosphorylation of Tyr was specified in SEQUEST and the phosphorylation of Tyr, Ser, and Thr was specified in X! Tandem as variable modifications.

Scaffold (Proteome Software Inc., Portland, OR; version Scaffold-01.06.05) was used to validate MS/MS-based peptide and protein identifications. Peptide identifications were accepted if they could be established at greater than 95.0% probability as specified by the Peptide Prophet algorithm (27). Protein identifications were accepted if they could be established at greater than 95.0% probability as assigned by the Protein Prophet algorithm (28). Proteins that contained similar peptides and could not be differentiated based on MS/MS analysis alone were grouped to satisfy the principles of parsimony. The assignment of post-translational modifications was made by the search engines (described above) and verified manually. Modification by sulfation was not distinguishable from phosphorylation with the mass accuracy of these experiments. However, these isobaric modifications were assumed to be phosphorylation if anti-Tyr(P) enrichment was used for peptide purification.

Label-free relative quantification was approached by two methods. In the first, differential abundance was estimated based on spectral counts; *i.e.* the total number of peptides identified by MS/MS and assigned to a protein. For a given protein, the total non-phosphorylated peptides from four experiments were summed, and values were normalized according to non-phosphorylated EGFR peptide spectral counts (29, 30). In the second, peak areas of SRM transitions were determined by using SRM Builder prototype software (Thermo Scientific; version 1.0) after confirming for each peptide the co-elution of all transitions. The most abundant transition for each peptide was used for quantification unless interference in this channel was observed (32). For those cases, the second most abundant transition was used. Noise levels were estimated based upon visual inspection

of signals preceding and following peptide peaks, and the signal-to-noise ratio was calculated by dividing peak intensity by the proximal noise (31). When the signal-to-noise ratio was less than 3 in a set of samples, these peptides were excluded in the protein quantification analysis.

SRM intensities for associated proteins were divided by the value measured for the EGFR normalization peptide YSFGATCVK (residues 285–293; see "Results") intrinsic to that sample. Hence calculated associated protein amounts are per unit of EGFR. The assumption was made that the amount of EGFR in cells did not change significantly after 15 min of EGF stimulation or SB-202190 incubation. Western blot results verified this assumption (*e.g.* Fig. 1*E*). Results from three independently repeated experiments were used to calculate statistical significance by the Student's *t* test. A complete listing of SRM intensities including coefficients of variance are included in the supplemental information.

The data described in this paper will be made freely available through databases including the Human Protein Reference Database, Human Proteinpedia, Global Proteome Machine, PhosphoELM, and PhosphoSite.

RESULTS

EGFR Variants Lacking Tyr(P)^{998} and Ser(P)^{991} Are Competent for EGFR → ERK Signaling but Defective for Endocytosis—The accumulation of phosphorylation at EGFR residue Tyr^{998} is documented to be relatively slow compared with other EGFR Tyr(P) sites when measured in HeLa cells (5), and our own experiments with HEK-EGFR cells are in agreement with these kinetics (data not shown). Similarly the kinetics of EGF-stimulated accumulation of a doubly phosphorylated EGFR peptide containing Ser(P)^{991} and Thr(P)^{993} was reportedly slow (10). In our experiments, the singly phosphorylated peptide containing Ser(P)^{991} was the most efficiently detected phosphoisomer of the MHLPSPTDSNFYR peptide.

The MS method of multiple reaction monitoring or SRM has been applied to quantify protein phosphorylation (32–34), including temporal analysis of Tyr(P) modifications associated with EGF treatment (8). The neutral loss of phosphoric acid from Ser(P) and Thr(P) sites is a frequent event during tandem MS of phosphopeptides (35–37), and the MS/MS spectrum of the EGFR tryptic peptide containing Ser(P)^{991} contained two prominent product ions representing loss of phosphoric acid from the parent ion and from the y10 fragment (Fig. 1*A*, see *arrows*). These neutral loss transitions were monitored as a means to measure Ser(P)^{991} following EGF stimulation of HEK-EGFR cells, and the duration of the EGF treatment was extended to 90 min (Fig. 1, *B* and *C*), which is longer than previous studies in which EGF-stimulated phosphorylation was monitored for up to 20 min post-EGF treatment (10). SRM analysis of neutral loss for phosphorylation measurement has been described previously (33). The SRM analysis indicated that the Ser(P)^{991} peptide increased ~10-fold after 90 min of EGF treatment and did not appear to reach a plateau or maximum by this time (Fig. 1*C*).

As a control, EGF-stimulated phosphorylation at EGFR Tyr^{1092}, which is associated with GRB2 binding and activation of RAS-ERK signaling, was monitored by Western immunoblotting (38). As expected, phosphorylation at this position was rapid and reached an apparent maximum by 1 min (Fig. 1*D*). It was observed that even 90 min after EGF stimulation there was not yet appreciable down-regulation of EGFR (Fig. 1*E*), which is typically more apparent by 4 h post-EGF (21). The relatively slow accumulation of phosphorylation at Ser^{991} following EGF treatment was pronounced and differs from the kinetics of the doubly phosphorylated isomer (Ser(P)^{991} with Thr(P)^{993}) described by Olsen *et al.* (10) that reached a maximum abundance near 10 min post-EGF and then receded to basal levels by 20 min. However, it is possible that the kinetics of these phosphorylations differ as a function of cell type and receptor densities, which are parameters that are different in our study and the comprehensive study by Olsen *et al.* (10).

The SRM measurements of the Ser(P)^{991} peptide were normalized to the amount of a non-phosphorylated EGFR peptide YSFGATCVK (residues 285–293) from the same sample. The signal for this control peptide was generated by summation of transitions precursor → y6 and precursor → y7 at corresponding time points of EGF stimulation (supplemental Fig. 1). The EGFR control peptide produced a high signal (intensity $>10^6$ units) and low coefficient of variation (CV = 8.3 ± 3.3%, $n = 9$) in test samples. Measurements of this peptide, therefore, were used as an indicator of EGFR amount in all SRM experiments in this study.

The relatively slow kinetics of phosphorylation at Ser^{991} and Tyr^{998} suggested that these modifications might not be involved in rapid signaling events associated with EGFR activation. To test this, site-directed mutagenesis was used to remove the side chain hydroxyl groups at these positions to prevent phosphorylation. Transfected HEK293 cell lines stably expressing variant proteins containing Tyr^{998}-to-Phe (EGFR Y998F) and Ser^{991}-to-Ala (EGFR S991A) at levels comparable to wild type (WT) EGFR in HEK-EGFR were established. These cell cultures were monitored for EGF-induced phosphorylation at Tyr^{1092} and for activation (phosphorylation) of the downstream MAP kinase ERK1/2. Phosphorylation of EGFR at Tyr^{1092} was unaffected by either Y998F or S991A substitution (Fig. 2, *A* and *B*), and the two mutant receptors did not show statistically significant changes in phosphorylated ERK1/2 following EGF treatment when compared with WT EGFR (Fig. 2, *C* and *D*).

To examine endocytosis of WT EGFR and the phosphorylation-defective receptor variants, localization of chimeric receptors containing carboxyl-terminal green fluorescent protein (GFP) was monitored by fluorescence microscopy. In serum-starved HEK-EGFR, HEK-S991A, and HEK-Y998F cells, the receptors were concentrated near the cell periphery consistent with plasma membrane localization (Fig. 3, *left panels*, *long arrows*). After exposure to 100 ng/ml EGF and incubation at 37 °C for 5 and 15 min, WT EGFR staining at the cell margins was diminished and became internalized and concentrated into intracellular aggregates characteristic of endosomes (Fig. 3, *upper row*, *short arrows*). By contrast,

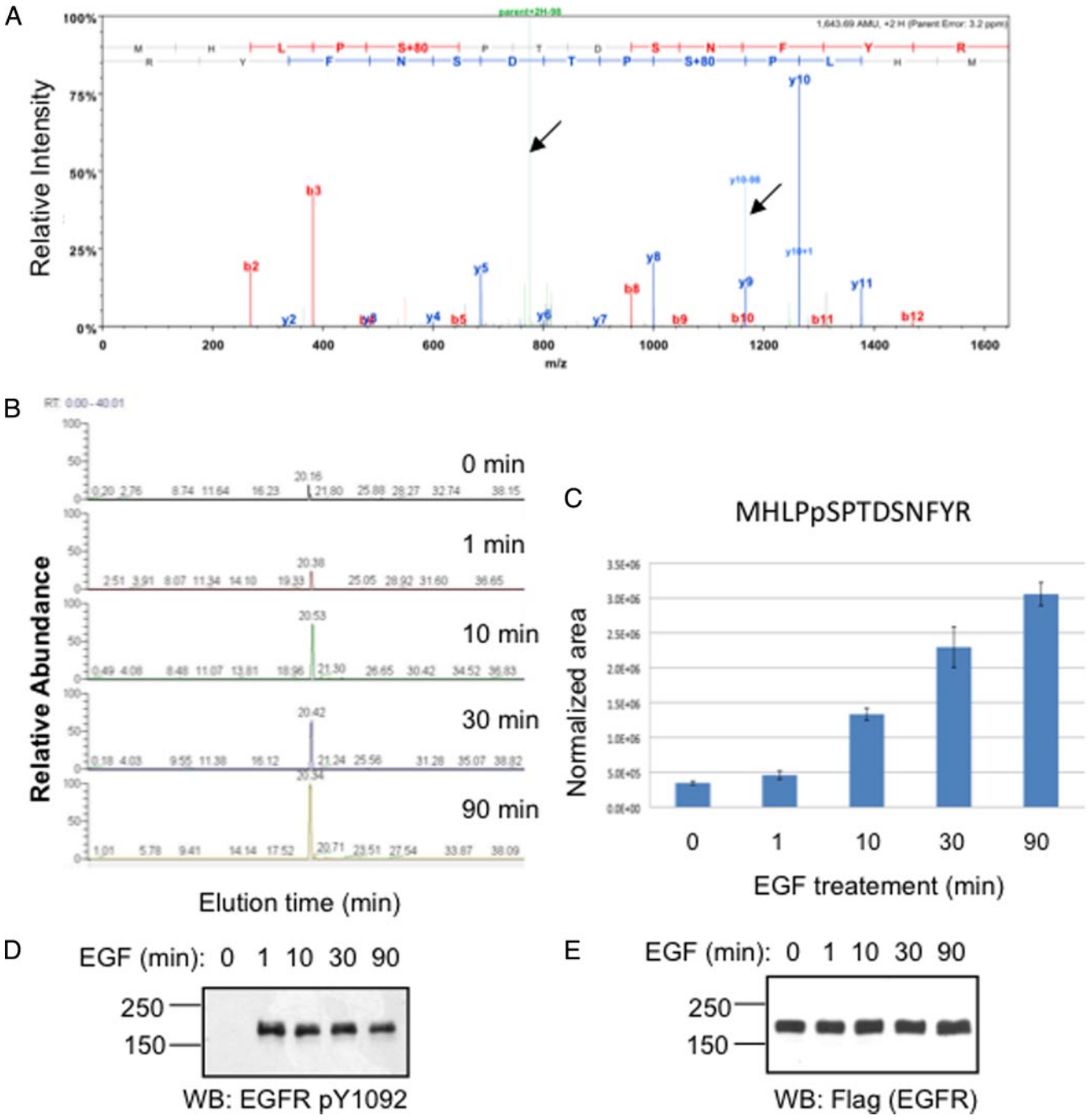

FIG. 1. **Detection and quantification of phosphorylation at EGFR Ser^{991} by SRM.** *A*, trypsin-digested immunopurified EGFR was analyzed by high resolution LC-MS/MS (Proxeon LC/source; Thermo LTQ-Orbitrap). The MS/MS spectrum of the EGFR peptide MHLPpS^{991}PTDSNFYR (where pS is phosphoserine) is shown (*upper panel*). The y and b series ions are indicated. *Arrows* point to product ions corresponding to parent − 98 and y10 −98 ions (as indicated), which reflect the neutral loss of phosphoric acid from the Ser(P) side chain. *B*, SRM LC elution profiles plotting the summed signal intensities of ions corresponding to singly phosphorylated MHLPSPTDSNFYR (precursor, m/z = 822.85, z = 2) transitioning to 1) precursor − 98/2 (m/z = 773.86, z = 2) and 2) y10 − 98 (m/z = 1165.50, z = 1) at various time points after EGF stimulation as indicated. *C*, histogram depicting the integrated SRM signal intensities normalized to a non-phosphorylated EGFR peptide in the same sample. *Error bars* indicate S.D. from three biological repeats of the experiment. *D* and *E*, Western blot (*WB*) analysis of whole-cell protein extracts from HEK-EGFR cells harvested following EGF treatment for the indicated durations. Antibodies specific to the EGFR phosphoepitope containing Tyr(P)^{1092} (*D*) or that recognize the FLAG epitope on EGFR-FLAG protein (*E*) were used to probe the filters, which were further developed with appropriate secondary antibody-enzyme conjugates and chemiluminescence imaging (see "Experimental Procedures"). *pY*, phosphotyrosine.

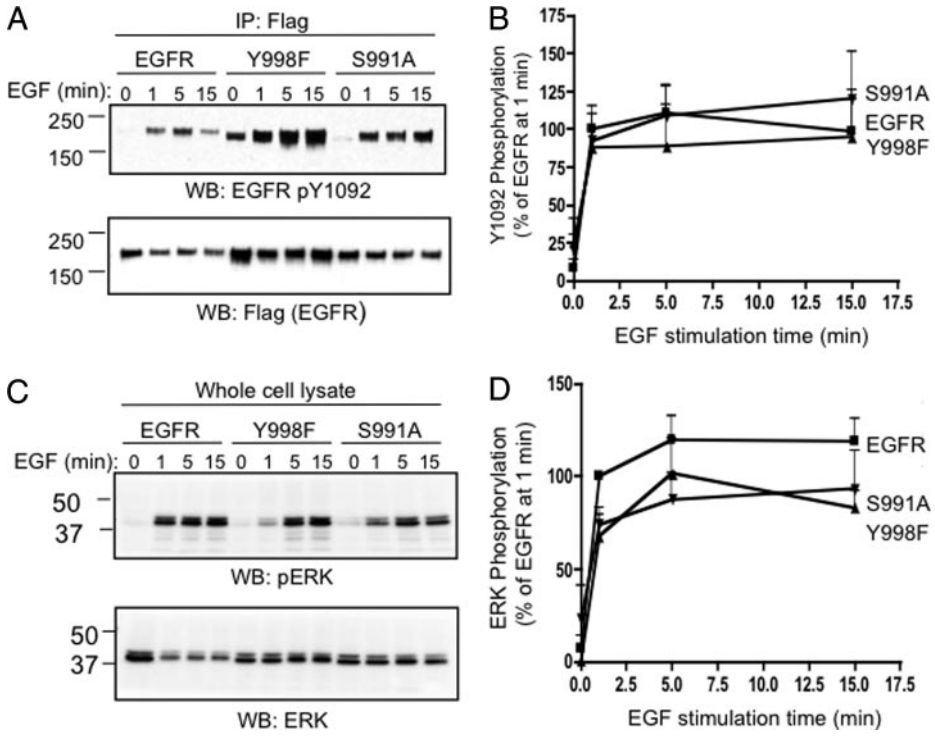

FIG. 2. **Phosphorylation of EGFR Tyr[1092] and ERK in EGF-stimulated HEK cells expressing wild type EGFR and the mutant receptors Y998F and S991A.** *A*, EGFR-FLAG proteins from HEK cells stably expressing wild type receptor (*EGFR*) or the indicated variants (Y998F and S991A) were isolated by immunoprecipitation (anti-FLAG) at the indicated times following cell stimulation with EGF, then resolved by SDS-PAGE, and subjected to immuno- (Western) blotting (*WB*) with the indicated anti-FLAG and anti-EGFR-Tyr(P)[1092] antibodies. *B*, the time course of phosphorylated EGFR Tyr[1092] after EGF stimulation from four biological repeats of the experiment shown in *A* and based on quantification of chemiluminescence light output. *C*, whole-cell lysates of the indicated cell samples prepared after the indicated durations of EGF treatment were blotted with antibodies directed against phosphorylated ERK (*pERK*; *upper panel*) and unphosphorylated ERK (*lower panel*). *D*, the time course of ERK phosphorylation after EGF stimulation from four biological repeats and quantified as described in *B*. The levels of EGFR Tyr(P)[1092] (*B*) and phospho-ERK (*D*) were normalized to their non-phosphorylated forms at corresponding time points, and the levels of phosphorylation after 1 min of EGF stimulation were arbitrarily regarded as 100%. *pY*, phosphotyrosine. *Error bars* indicate S.D. from four independent experiments.

Y998F and S991A mutant receptors displayed far less internalization/aggregation and remained largely concentrated at the cell periphery (Fig. 3, *middle* and *lower rows*, *long arrows*). These observations demonstrate defective endocytosis of the mutant receptors. The endocytosis defect of EGFR Y998F is expected based on Sorkin *et al.* (16). The cell staining was categorized into two types: WT-like, typified by internalized and aggregated receptors and little or no staining at the cell margins, and mutant-like, which lacked intracellular aggregates and retained concentrated staining at the cell margins. After tabulating these patterns in 100 cells in three separate experiments, ~60% of WT receptors displayed the WT-like pattern of internalized receptors (diminished peripheral staining accompanied by internalized aggregates), whereas only ~30% of Y998F and 25% of S991A receptors showed this pattern.

To further examine and to quantify the extent of EGF-stimulated receptor internalization, cells were treated with or without EGF for 30 min, and then receptors exposed on the cell surface were covalently labeled with biotin. Receptors were then purified by immunoprecipitation and quantified for biotinylation by Western blotting with a streptavidin probe (Fig. 4*A*). After EGF treatment, the amount of surface-exposed, biotinylated WT EGFR was decreased by ~50%, whereas the amounts of surface exposed Y998F and S991A receptors were almost equivalent to levels in untreated cells (Fig. 4*A*). As an additional measure of receptor endocytosis, receptor-mediated internalization of rhodamine-labeled EGF was measured by flow cytometry. As shown in Fig. 4*B*, ligand internalization by Y998F and S991A was less than that observed for WT EGFR. Therefore, by three different measures, the Y998F and S991A variants were defective for receptor endocytosis.

EGFR-associated Proteins and Phosphorylation—To further address the function of the kinase domain proximal phosphorylation sites at Ser[991] and Tyr[998], receptor-associated proteins and receptor phosphorylation were examined by using LC-MS/MS and in some instances quantified by SRM. Tandem MS analysis served three purposes. First, it enabled the identification of receptor-associated proteins, which could then be compared with a reference set of EGFR-associated proteins. Second, it facilitated the measurement of spectral counts as a

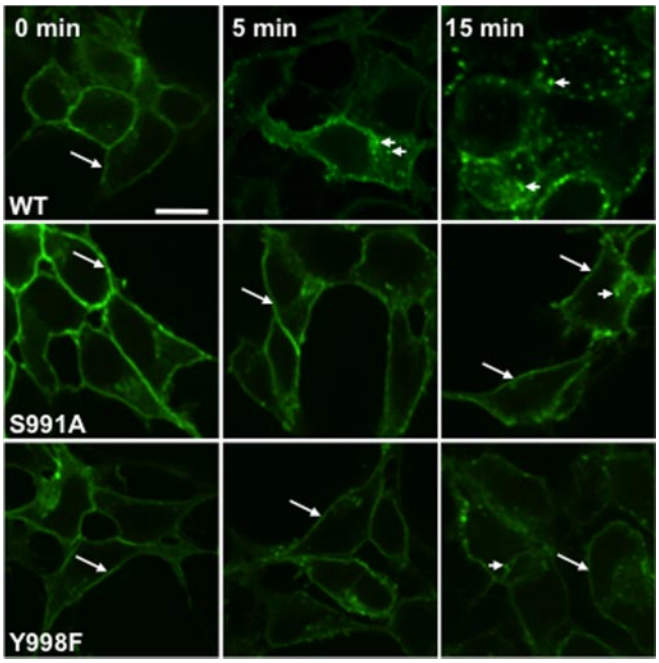

FIG. 3. **Spatial and temporal dynamics of wild type EGFR and phosphorylation-deficient variants.** HEK293-based cells stably expressing WT, S991A, and Y998F EGFR proteins (as indicated) fused to GFP were treated with EGF (100 ng/ml) for 0, 5, and 15 min at 37 °C as indicated, then fixed, and localized by using fluorescence microscopy. *Long arrows* indicate staining at the cell periphery near plasma membranes, and the *short arrows* indicate regions of aggregated intracellular staining that may correspond to the endosomal compartment. *Scale bar*, 100 μm.

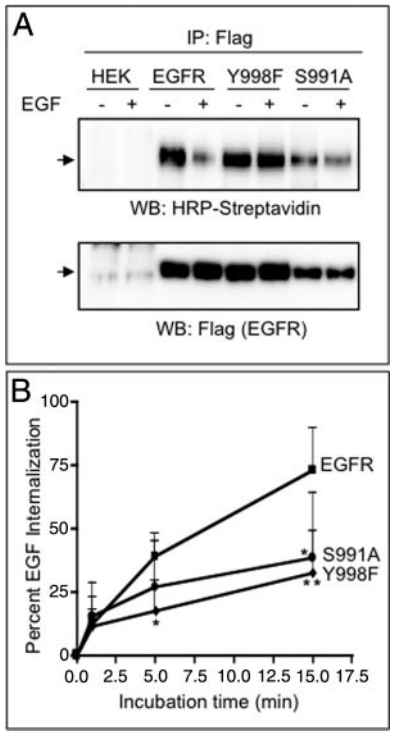

FIG. 4. **Quantification of EGFR endocytosis.** *A*, the level of surface-exposed EGFR in the indicated cell lines was measured before (−) and after (+) EGF (50 ng/ml) was added to serum-starved cells for 30 min at 37 °C. Treated cells were then surface-labeled with biotin (30 min, 23 °C), and EGFR proteins were recovered by IP and Western blotted (*WB*) with FLAG antibodies to reveal total EGFR-FLAG (*lower panel*) and with a horseradish peroxidase-streptavidin conjugate to identify biotin-labeled receptors (*upper panel*). *B*, fluorescence-activated cell sorting analysis was used to quantify the time course of internalization of rhodamine-EGF by cells expressing the indicated WT and variant EGFR proteins. Both variant proteins were statistically different from WT (*, $p = 0.05$; **, $p = 0.01$). *Error bars* indicate S.D. from four independent experiments.

first approximation of protein abundance (39). Third, it provided information on peptides and their fragmentations, which were useful in the design of SRM methods for the quantification of receptor-associated proteins in repeated experiments.

EGFR immunoprecipitates from EGF-stimulated cells expressing WT and variant EGFR proteins were prepared by using anti-FLAG antibodies and analyzed by LC-MS/MS for associated proteins similar to previously published methods involving gel-free, LC-MS/MS analysis of trypsin-digested, anti-FLAG immunoprecipitates (22, 40). In aggregate 444 proteins were identified in the anti-FLAG immunoprecipitates of WT and mutant receptors by using criteria described under "Experimental Procedures" (*i.e.* at least two distinct peptides and 95% probability scores by Peptide Prophet and Protein Prophet algorithms (27, 28)). Not surprisingly, this list (supplemental Table 1) contains proteins commonly known to associate with FLAG immunoprecipitates (40). To focus the analysis of receptor-associated proteins, the list was compared with data from the manually curated Human Protein Reference Database, which lists 144 EGFR-binding proteins that have experimental validation in the literature. Table I shows the 17 proteins, in addition to the EGFR, that intersect these two data sets including the ligand EGF; proteins involved in EGFR signaling such as SHC1, GRB2, and SOS1; and others associated with receptor endocytosis, including the ubiquitin E3 ligases CBL and CBLB and ubiquitin (Table I).

The spectral counts of these EGFR-associated proteins were noted as a crude measure of their abundance in the IP samples. Spectral counts were normalized by adjusting for the number of spectral counts from non-phosphorylated EGFR peptides. EGFR peptides, as expected, were by far the most abundant class of peptide in the samples (Table I), and this observation served to validate that the IP method was specific for this antigen. For each of the proteins mentioned above, VAV2, and the phosphatidylinositol 3-kinase p85 subunits (PIK3R1 and PIK3R2), spectral counts associated with WT EGFR increased as a consequence of EGF treatment of cells. Furthermore with the exception of EGF and CBLB, the spectral counts for these proteins measured with EGF-stimulated Y998F and S991A receptors were less than those observed for WT (Table I).

To quantify the receptor-associated proteins, including changes due to EGF stimulation and as a consequence of the

TABLE I
EGFR-associated proteins

Proteins identified in EGFR immunoprecipitates are listed according to their IPI number, protein name, and molecular weight as indicated. Percent sequence coverage and protein identification probability according to the Protein Prophet algorithm (29) are also shown. LC-MS/MS analysis (LTQ-Orbitrap) was performed with trypsin-digested EGFR immunoprecipitates from unstimulated WT EGFR-expressing cells (Cont) and EGF-stimulated cells expressing WT EGFR (EGFR), Y988F variant (Y988F), and S991A variant (S991A). Spectral counts (columns 6–9) are the total number of spectra, including repeat identifications, of peptides derived from the indicated proteins. The spectral counts in each column were normalized by a factor such that the number of unphosphorylated EGFR-derived peptides (shown in the top row) were equalized to the value obtained for the EGFR sample. The actual number of non-phosphorylated, receptor-derived peptides is shown in parentheses. Note that the accession number for EGF corresponds to the 1207-residue pre/pro-EGF protein, whereas the degree of coverage, corresponding to residues 971–1011, relates to overlap within the 53-residue, processed growth factor (residues 971–1023).

Accession no.	Protein name	Molecular weight	Sequence coverage	Identification probability	Spectral counts[a]			
					Cont	EGFR	Y998F	S991A
			%	%				
IPI00018274	EGFR unphosphorylated peptides (non-normalized EGFR peptides)	134,245	71	100	892 (1,131)	892 (892)	892 (1,127)	892 (1,284)
IPI00027269	CBL	99,631	44	100	42	172	95	54
IPI00021327	GRB2	25,189	72	100	77	139	104	75
IPI00020131	SOS1	152,451	51	100	107	133	68	37
IPI00021326	SHC1	62,876	44	100	27	74	46	23
IPI00004977	VAV2	97,017	24	100	12	41	7	3
IPI00292856	CBLB	109,435	36	100	8	17	26	17
IPI00179330	Ubiquitin (UBB)	17,948	48	100	11	16	8	8
IPI00011736	PIK3R2	81,608	17	100	0	12	3	2
IPI00017963	SNRPD2	13,509	41	100	9	8	13	10
IPI00008603	ACTA2	41,992	27	99.0	8	7	8	5
IPI00000073	EGF	6,045	77.4	100	0	6	11	7
IPI00021448	PIK3R1	83,583	10	100	1	6	0	1
IPI00004399	Mig6	50,543	11	99.9	7	4	6	4
IPI00395769	ATP5C1	32,865	21	100	7	4	5	3
IPI00017510	MT-CO2	25,548	8.8	99.4	4	2	0	0
IPI00021263	14-3-3 ζ/δ	27,728	15	99.0	3	2	4	2
IPI00020134	SOS2	153,019	11	100	5	1	5	3

[a] Normalized to EGF-stimulated WT EGFR.

Y998F and S991A mutations, SRM analysis was applied to the receptor·immunoprecipitate complexes isolated from cells before and after EGF treatment. An SRM method that tracked the top six EGFR-associated proteins (according to spectral counts associated with WT EGFR; Table I) was formulated based on transitions summarized in supplemental Table 2. The fragmentation patterns obtained during discovery analyses with the LTQ-Orbitrap were a useful starting point toward the development of the SRM transitions. However, the resonance excitation-based fragmentations produced in the linear ion trap were not identical with the true CIDs undertaken in Q2 of the triple quadrupole TSQ instrument that was used for SRM. The intensity of b ions was generally greater in the linear ion trap, which also had a low molecular weight cutoff (*i.e.* ⅓ rule) that made low *m/z* ions more predominant in the triple quadrupole TSQ instrument. In addition, the LC gradients were of different durations (120 min with the Orbitrap and 40 min with the TSQ instrument). The SRM method was applied in three independent biological experiments resulting in the quantification the EGFR and the six receptor-associated proteins (Fig. 5 and Table II). The EGFR peptide YSFGATCVK (residues 285–293; described above), which is common to the WT and variant proteins and not subject to phosphorylation, was quantified and used to normalize for the amount of EGFR in each sample.

The interactions of all six proteins were verified by the SRM analysis (Fig. 5). The largest EGF-stimulated -fold increases in receptor binding were observed for CBL followed by GRB2. CBL association with WT EGFR increased more than 7-fold following EGF treatment but was less than 5-fold with S991A and was ~4-fold with the Y998F variant. The drop in CBL association associated with the Y998F mutation was significantly different from WT ($p = 0.01$; Fig. 5). EGF-stimulated receptor association of GRB2 was roughly 3-fold, which was a statistically significant increase over that observed without EGF treatment, and the measurements for GRB2 were not different between WT and the variant receptors (Fig. 5). The associations of VAV2 and SOS1 were measured to be essentially constitutive and unaffected by the phosphorylation site mutations because no statistically significant differences were noted following EGF treatments or between the WT and the variant receptors (Fig. 5). The binding of SHC1 to WT EGFR was stimulated more than 2-fold by EGF, but for the receptor variants, EGF-stimulated SHC1 association was associated with too much variation to be considered significant. The capture of ubiquitin with WT and Y998F was increased more than 3-fold by EGF but to a lesser extent with the S991A variant. Furthermore with EGF-treated cells the amount of receptor-associated ubiquitin was significantly reduced in S991A

compared with WT (Fig. 5). Table II shows the peptides, SRM transitions, and coefficients of variance associated with the data depicted in Fig. 5. A more complete listing of these measurements including SRM intensities for each of the three repeated experiments is provided in supplemental Table 4.

The observed changes in receptor-associated CBL and ubiquitin were supported by Western blot analysis (Fig. 6). The variant receptors were not generally impaired for phosphorylation at the CBL binding site Ser(P)^{1069}, but the Y998F and S991A protein complexes captured by anti-FLAG IP were observed to contain less CBL and ubiquitin than did WT (Fig. 6). The co-immunoprecipitation of ubiquitin may reflect the ubiquitination of any of the proteins in the receptor (anti-FLAG) immunoprecipitates. However, prominent anti-ubiquitin immunostaining was concentrated at or slightly above the migration of the receptors, suggesting that ubiquitination of the receptors, as expected (19), may account for a portion of the ubiquitin measured by MS.

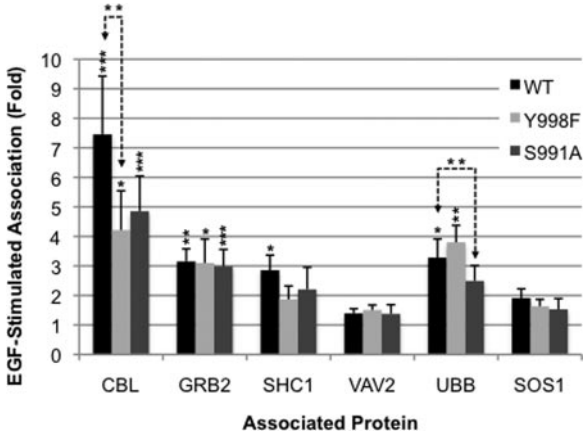

FIG. 5. **SRM-based measurement of EGFR-associated proteins.** EGFR was recovered by anti-FLAG IP from HEK cells stably expressing WT EGFR or one of the variants Y998F or S991A. The immune complexes were converted to tryptic peptides, which were subjected to SRM analysis to specifically monitor transitions derived from the indicated EGFR-associated proteins (see Table II). Protein amounts are expressed per unit of EGFR protein after normalization with an intrinsic EGFR peptide (see "Experimental Procedures"). Protein amounts are shown as EGF-induced -fold increases relative to unstimulated cells (means ± S.E., $n = 3$). For the purpose of constructing the histogram, values from unstimulated (*i.e.* no EGF) cells were set to unity; however, variation associated with all measurements were included in Student's *t* test calculations. *Asterisks above bars* indicate statistically significant differences from the amount of receptor-associated protein measured with unstimulated cells (*, $p = 0.05$; **, $p = 0.01$; ***, $p = 0.005$). Additionally the level of receptor association achieved by each of the proteins in EGF-stimulated cells was compared and found to be statistically different from WT (**, $p = 0.01$) only for CBL and ubiquitin (*UBB*) as indicated by the *dashed lines*.

The level of endogenous EGFR in HEK293 cells is very minor (22), and association with other ErbB family receptors was not detected. This indicated that dimerization of FLAG-tagged ectopic receptors with endogenous ErbB family members to which associated proteins might bind was not a factor in these experiments.

Among the peptides characterized by LC-MS/MS analysis of EGFR immunoprecipitates were phosphopeptides. Following EGF stimulation, the total number of spectral counts for EGFR-derived phosphorylated peptides was 69 for WT EGFR, 72 for the Y998F variant, and 73 for S991A. Thus, by this estimation the mutants missing one or another kinase domain proximal phosphorylation site were not generally impaired for phosphorylation. As shown in Table III, there is evidence for phosphorylation at 18 sites on the receptor, including three Thr(P), six Tyr(P), and nine Ser(P). Additional information related to these assignments including protein search algorithm scores and MS/MS spectra are included in supplemental Table 3 and supplemental Fig. 2. The low number of observed phosphopeptides was not surprising because no phosphopeptide enrichment was used in this analysis. For several sites, the number of observed spectra was too low to warrant further discussion.

Surprisingly in the region spanning EGFR residues 1000–1052 there was evidence for increased phosphorylation with the Y998F and S991A variants (see bold region in Table III). There were, respectively, 20 and 23 phosphorylated peptides identified by spectral counting for these variants but only six

TABLE II

SRM-based measurement of six EGFR-associated proteins

Cells stably expressing FLAG-tagged wild type receptor (EGFR) or the S991A and Y998F EGFR proteins (as indicated) were treated with or without EGF (100 ng/ml) for 15 min at 37 °C. Anti-FLAG immune complexes were digested with trypsin and analyzed by SRM (see "Experimental Procedures"). Protein name and peptide sequence are indicated in the first two columns, respectively. The third column indicates the *m/z* values for the Q1-to-Q3 transitions that were monitored. In columns 4–12, the EGF-induced -fold change in abundance of associated proteins is indicated for the WT EGFR and the indicated variant receptors. -Fold changes are presented as the mean of $n = 3$ independent experiments with CV and S.E. and correspond to the histogram presented in Fig. 5.

Protein	Peptide	Q1/Q3 transition	WT			Y998F			S991A		
			Mean	CV	S.E.	Mean	CV	S.E.	Mean	CV	S.E.
CBL	GTEPIVVDPFDPR	721.37/631.3	7.46	0.46	1.97	4.21	0.55	1.33	4.86	0.42	1.19
GRB2	FNSLNELVDYHR	753.87/802.4	3.15	0.23	0.42	3.10	0.45	0.81	2.99	0.33	0.57
SHC1	GLLVPALK	405.78/428.3	2.85	0.31	0.51	1.87	0.42	0.45	2.21	0.59	0.75
VAV2	HLLLVDPEGVVR	673.89/656.4	1.40	0.19	0.16	1.51	0.19	0.17	1.38	0.39	0.31
UBB	SHASGTYLIR	552.79/880.5	3.28	0.33	0.63	3.80	0.26	0.57	2.49	0.36	0.52
SOS1	TITLEVEPSDTIENVK	894.47/1131.6	1.91	0.28	0.31	1.63	0.25	0.23	1.53	0.41	0.36

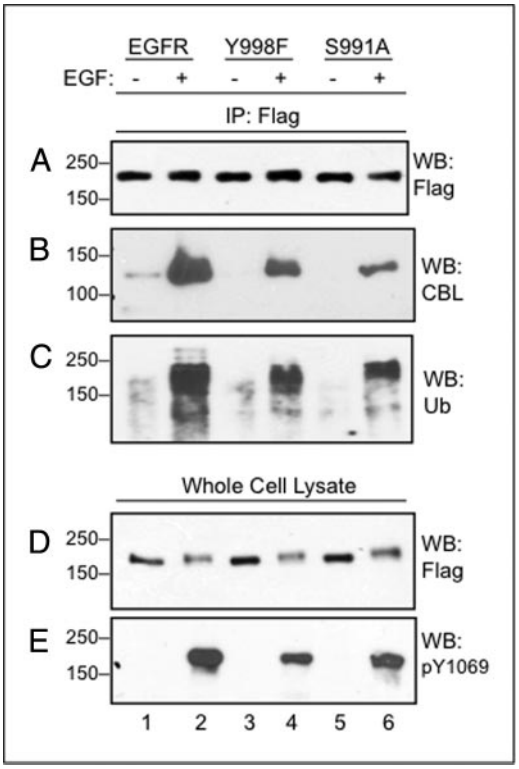

FIG. 6. **Western blot analysis of EGFR and associated proteins.** FLAG-tagged wild type receptor (*EGFR*) and the variants Y998F and S991A, as indicated, were collected by anti-FLAG IP from total cell lysates prepared from cells treated without or with EGF (15 min, 37 °C, 100 ng/ml; see "Experimental Procedures"). Following SDS-PAGE and electrophoretic transfer, filters were developed with antibodies to FLAG (*A*), CBL (*B*), and ubiquitin (*Ub*; *C*). A portion of the lysates was analyzed without IP for FLAG (*D*) and the CBL binding site at phosphorylated EGFR residue Tyr^{1069} (*E*). Shown are representative results from repeated experiments. *WB*, Western blot; *pY*, phosphotyrosine.

in the case of WT (Table III). Most notable were phosphorylations at positions Thr^{1041} and especially Ser^{1039} for which spectral counts were higher in the two receptor variants than in WT (Table III). Both of these phosphorylations were observed previously in EGF-stimulated HeLa cells (10). These sites reside in the same tryptic peptide spanning residues 1032–1052. This peptide was also detected doubly phosphorylated at $Ser(P)^{1039}$ and $Ser(P)^{1041}$, but the ion current intensities were relatively low (data not shown).

The monophosphorylated isobaric isomers containing either $Ser(P)^{1039}$ or $Thr(P)^{1041}$ were analyzed by LC-MS/MS, which confirmed their identities. For example, their y12 fragment ions were clearly distinctive (Fig. 7, *A* and *B*). The two species did not co-elute during reverse phase chromatography, and this facilitated their resolution and ion current measurement by high resolution LC-MS (Fig. 7*C*). To facilitate the quantification of these species by SRM, the measurement of transitions involving distinctive y ions was attempted but proved inefficient. Therefore, an optimized SRM method was developed that included neutral loss of phosphoric acid (*i.e.* doubly charged parent − 98/2) and y5-associated transitions, which were common to the two phosphoisomers and efficiently detected (Fig. 7, *A*, *B*, and *D*). Note that different elution gradients were used for the LC-MS and SRM analyses shown in Fig. 7, *C* and *D*, respectively, so the retention times were not identical. The Orbitrap MS extracted ion current chromatograph and triple quadrupole SRM traces were similar (Fig. 7, compare *C* and *D*), and several repeats of the LC-MS/MS experiment indicated that the $Ser(P)^{1039}$ peptide consistently eluted immediately before the $Thr(P)^{1041}$ isomer.

Having established the SRM method, it was applied to quantify phosphorylation at Ser^{1039} and Thr^{1041} and address three questions: first, to determine whether these modifications were affected by EGF ligand; second, to determine whether they were elevated with the Y998F and S991A variant receptors compared with WT as implied by the semiquantitative spectral counting analysis shown in Table III; and third, to determine whether these modifications require p38 kinase. Stress (*e.g.* TNFα or UV irradiation)-induced p38 kinase-dependent phosphorylation within the Ser/Thr-rich segment of the EGFR spanning residues 1026–1046, but not at Ser^{1039} specifically, was shown by Zwang and Yarden (17). Fig. 7, *E* and *F*, present a summary of three independent repeats of an experiment that addressed these questions. Stimulation of cells with EGF caused an ~3-fold elevation in the abundance of the $Ser(P)^{1039}$ peptide (3.4 ± 1.3 S.D.) (Fig. 7*E*), whereas both the Y998F and S991A variants showed a roughly 10-fold elevation in the abundance of the $Ser(P)^{1039}$ peptide after EGF treatment. The pronounced EGF-stimulated increase in $Ser(P)^{1039}$ was largely eliminated by treatment of cells with SB-202190, which is a potent inhibitor of MAP kinases p38α/β (23), indicating that these phosphorylation sites are regulated by p38 kinase (Fig. 7*E*). A similar phenomenon was observed for $Thr(P)^{1041}$ wherein EGF treatment stimulated $Tyr(P)^{1041}$ more than 2-fold in WT (2.7 ± 1.1 S.D.) but to an even greater extent with the variants (Fig. 7*F*). The Thr^{1041} modifications were also sensitive to the p38 inhibitor (Fig. 7*F*).

DISCUSSION

EGFR Mutants Y998F and S991A Signal to ERK but Are Defective in Endocytosis—Cellular responses to EGFR activation occur with different kinetics, and to some extent this reflects temporal regulation of receptor and substrate phosphorylation and the dynamics of receptor trafficking and protein-protein interactions (3, 9, 10). The phosphorylations of EGFR at Ser^{991} and Tyr^{998} were found in tumors as sites modulated by EGF and an EGFR kinase inhibitor, suggesting their involvement in EGFR regulation and/or signaling (10, 12). In this study and other published reports (10) EGF-stimulated phosphorylations at these sites occurred with relatively slow kinetics and in this study were found not to be required for downstream ERK activation, which suggests that their function is not required for signaling along the RAS-ERK axis.

TABLE III

EGFR phosphorylation site analysis suggests increased levels of EGF-induced phosphorylation compared with WT at Ser[1039] and Thr[1041] in the Y998F and S991A variants

The indicated FLAG-tagged receptor proteins were recovered by IP from unstimulated WT EGFR-expressing cells (Cont) and EGF-stimulated cells expressing WT EGFR (EGFR), Y988F variant (Y988F), and S991A variant (S991A). The immune complexes were digested with trypsin, and peptides were analyzed by LC-MS/MS. Total spectral counts, peptide sequences, and phosphosites are indicated. The bold area includes a Ser/Thr-rich region spanning 1026–1046 previously implicated to contain p38 MAP kinase phosphorylation sites (18) and includes peptides containing Ser(P)[1039] and Thr(P)[1041]. pS, phosphoserine; pT, phosphothreonine; pY, phosphotyrosine.

EGFR peptide sequence	Residue	Spectral counts			
		Cont	EGFR	Y998F	S991A
R ↓ ELVEPLpTPSGEAPNQALLR ↓ I	Thr(P)[693]	5	13	8	11
R ↓ MHLPpSPTDSNFYR ↓ A (EGFR)	Ser(P)[991]	0	2	0	0
R ↓ MHLPpSPTDSNFFR ↓ A (Y998F)	Ser(P)[991]	0	0	8	0
R ↓ ALMDEEDMDDVVDADEYLIPQQGFFSpSPSTSR ↓ T	**Ser(P)[1026]**	1	**1**	**1**	**3**
R ↓ TPLLSpSLSATSNNSTVACIDR ↓ N	**Ser(P)[1037]**	0	**0**	**1**	**1**
R ↓ TPLLSSLpSATSNNSTVACIDR ↓ N	**Ser(P)[1039]**	2	**3**	**10**	**13**
R ↓ TPLLSSLSApTSNNSTVACIDR ↓ N	**Thr(P)[1041]**	3	**2**	**8**	**6**
R ↓ pYSSDPTGALTEDSIDDTFLPVPEYINQSVPK ↓ R	Tyr(P)[1069]	0	3	1	5
R ↓ YSSDPTGALTEDpSIDDTFLPVPEYINQSVPK ↓ R	Ser(P)[1081]	0	0	1	0
R ↓ YSSDPTGALTEDSIDDpTFLPVPEYINQSVPK ↓ R	Thr(P)[1085]	0	1	0	0
R ↓ YSSDPTGALTEDSIDDTFLPVPEpYINQSVPK ↓ R	Tyr(P)[1092]	3	1	4	5
R ↓ YSSDPTGALTEDSIDDTFLPVPEYINQpSVPK ↓ R	Ser(P)[1096]	1	1	0	0
K ↓ RPAGpSVQNPVYHNQPLNPAPSR ↓ D	Ser(P)[1104]	0	1	0	2
K ↓ RPAGSVQNPVpYHNQPLNPAPSR ↓ D	Tyr(P)[1110]	4	5	4	3
R ↓ DPHYQDPHSTAVGNPEpYLNTVQPTCVNSTFDSPAHWAQK ↓ G	Tyr(P)[1138]	1	4	0	1
K ↓ GSHQIpSLDNPDYQQDFFPK ↓ E	Ser(P)[1166]	9	11	6	6
K ↓ GSHQISLDNPDpYQQDFFPK ↓ E	Tyr(P)[1172]	8	14	14	10
K ↓ GSHQIpSLDNPDpYQQDFFPK ↓ E	Ser(P)[1166], Tyr(P)[1172]	1	0	0	0
K ↓ GSTAENAEpYLR ↓ V	Tyr(P)[1197]	2	7	6	7
Total peptide number		40	69	72	73

Indeed the results from three different assays indicated that the phosphorylation-deficient variants S991A and Y998F were defective in receptor endocytosis. These data indicate that to some extent signaling may proceed independently of normal receptor trafficking.

Our data indicate that EGFR endocytosis is subject to regulation involving the phosphorylation of Tyr[998] and amino-terminal to it at Ser[991]. Sorkin *et al.* (16) described Tyr[998] as part of a tyrosine-based internalization motif. Indeed the structural analysis by Owen and Evans (41) of an EGFR peptide containing this residue (FYRALM) bound to the endocytosis adaptor protein adaptin $\mu 2$ showed Tyr[998] and Leu[1001] tightly bound in pockets and predicted that phosphorylation at Tyr[998], which was not yet appreciated, would prevent the receptor-$\mu 2$ interaction. The cell adhesion molecule L1 contains a tyrosine-based endocytosis motif (YRSL) similar to the EGFR Tyr[998] motif (YRAL). In L1, tyrosine phosphorylation of the motif appears to modulate L1 interactions with adaptin AP-2 as a requisite for clathrin-mediated endocytosis (42). We did not identify adaptins as EGFR-associated likely because our buffers lacked deoxycholate as a reagent necessary for the detection of the EGFR·AP-2 complex (16). A more detailed analysis of the subcellular localization of Y998F and S991A receptor variants may provide more insight into the function of the 998 and 991 phosphorylation sites and mechanisms of EGFR trafficking.

Given the slow kinetics of Tyr[998] and Ser[991] phosphorylation, in the case of Ser(P)[991] still accumulating 90 min after EGF (Fig. 1), it is possible these modifications are not required for receptor internalization *per se* but may play a role at a later stage of endocytosis. For example, phosphorylation at these sites may promote dissociation of proteins from internalized receptors that would otherwise impair subsequent trafficking. Our findings do not indicate the full nature of the receptor endocytosis defect associated with the variant receptors nor the extent to which this phenotype is a consequence of the side chain substitutions or their lack of phosphorylation but clearly establish a role for Ser[991], in addition to the known requirement for Tyr[998] (16), in EGFR endocytosis. This study did not aim to identify the kinase(s) responsible for the phosphorylations at Tyr[998] and Ser[991]. Given evidence that EGFR endocytosis does not require EGFR kinase activity (26), we predict that the Tyr[998] kinase is not the EGFR itself. Again this is consistent with Tyr[998] phosphorylation accumulating after the initial wave of EGFR autophosphorylation events (10).

Quantification of EGFR-associated Proteins and Phosphorylation by SRM—The results obtained by SRM-based examination of a limited set of receptor-associated proteins are consistent with the conclusion that the S991A and Y998F variants are defective in EGFR endocytosis. Among the six well established EGFR-associated proteins examined, the ubiquitin E3 ligase CBL and ubiquitin itself were found to differ from WT with one or the other endocytosis-defective receptor variant. Ubiquitin and CBL have defined roles in the down-regulation of EGFR and other receptor tyrosine kinases (19, 43–45). Western blot analysis confirmed the diminished association of CBL with the activated variant receptors com-

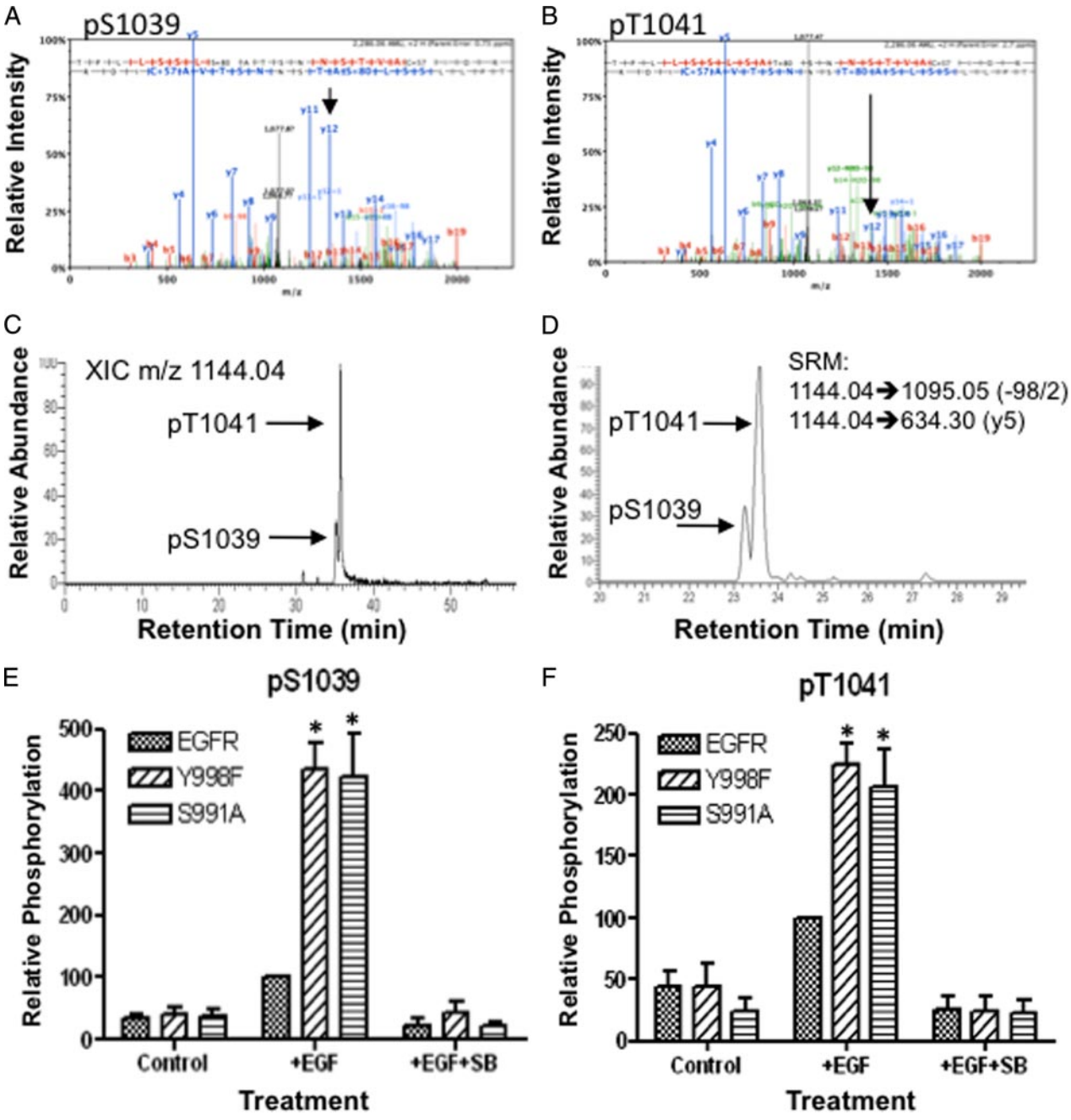

FIG. 7. **Detection and quantification of phosphorylation at EGFR Ser[1039] and Thr[1041] by LC-MS/MS and SRM.** *A* and *B*, trypsin-digested immuno (anti-FLAG) purified EGFR proteins were analyzed by high resolution LC-MS/MS. MS/MS spectra of the EGFR peptide TPLLSSLpS[1039]ATSNNSTVACIDR (where pS is phosphoserine) (*A*) and TPLLSSLSApT[1041]SNNSTVACIDR (where pT is phosphothreonine) (*B*) are shown. The y and b series ions are indicated. *Arrows* point to product y12 ions. As expected the *m/z* values of y12 ions are different between Ser(P)[1039] (*A*) and Thr(P)[1041] (*B*) peptides because Thr[1041] or Thr(P)[1041] is the amino-terminal residue in the y12 ions. *C*, the orbitrap XIC for the isobaric phosphopeptides with *m/z* 1144.04 and containing Ser(P)1039 or Thr(P)1041, as indicated, are shown to be chromatographically resolved. *D*, SRM LC elution profiles plotting the summed signal intensities of ions corresponding to singly phosphorylated TPLLSSLSATSNNSTVACIDR (precursor, $m/z = 1144.04$, $z = 2$) transitioning to 1) precursor − 98/2 ($m/z = 1095.05$, $z = 2$) and 2) y5 ($m/z = 634.30$, $z = 1$) as indicated. *E* and *F*, histograms depicting the integrated SRM signal intensities of Ser(P)[1039] peptide (*E*) and Thr(P)[1041] peptide (*F*) normalized to a control EGFR peptide in the same sample (see "Experimental Procedures"). EGFR, Y998F, and S991A cell cultures were treated without (*Control*) or with (+*EGF*) EGF (100 ng/ml, 15 min, 37 °C) or with EGF after a 30-min pretreatment with the p38 inhibitor SB-202190 (10 μM) (+*EGF*+*SB*). *Error bars* indicate S.D. from three biological repeats of the experiment. For statistical analysis, Y998F and S991A samples were compared with wild type EGFR in EGF-stimulated samples (+*EGF*), and EGFR, Y998F and S991A samples in SB-202190 treated cells (+*EGF*+*SB*) were compared with themselves in EGF-stimulated samples (+*EGF*). *, $p = 0.05$ compared with wild type EGFR +EGF. In all cases phosphopeptides were statistically significantly less ($p = 0.05$) for control and SB-202190-treated samples compared with cognate +EGF samples. *XIC*, extracted ion current.

pared with WT and demonstrated that the mutant receptors remained competent for phosphorylation at Tyr^{1069}, which is the direct binding site on the receptor for CBL. GRB2 is required for EGFR endocytosis (24, 46–49). In addition, it interacts with SHC and SOS1/2 as effectors of RAS and ERK downstream of activated tyrosine kinases (50). The EGFR variants Y998F and S991A retained both EGF-stimulated phosphorylation at the principal GRB2 binding site Tyr^{1092} (38) and GRB2 association in amounts not significantly different from WT. This further indicates that the early stages of ligand-stimulated receptor activation were not impaired by the Y998F and S991A mutations and that the endocytosis defects associated with Y998F and S991A are not a consequence of impaired GRB2 bindings to the receptors.

The EGF-stimulated increase in receptor-associated ubiquitin displayed by the variant receptors (although for S991A it was less than that of WT) is consistent with the conclusion that to some extent they did become internalized. However, our data do not address which proteins in the receptor complexes were covalently modified by ubiquitin.

A Link between EGFR Recycling and Degradation Pathways—Our data revealed an unforeseen connection between the pathways of EGFR recycling and down-regulation. The p38 MAP kinase-dependent phosphorylations at Ser^{1039} and Thr^{1041} in the endocytosis-defective variants were pronounced. Because the phosphorylations at Ser^{1039} and Thr^{1041} were EGF-stimulated, we conclude they are a normal part of the EGF response and that the Y998F and S991A mutations do not themselves constitute a "stress" that induced the recycling response in cells. Unmapped p38-dependent phosphorylation(s) in a 21-residue segment of the receptor (spanning 1026–1046) that includes these residues was shown previously to be required for EGFR recycling following cell treatments including TNFα, osmotic stress, UV irradiation, and the chemotherapeutic agent cisplatinum but was not linked to EGF ligand-stimulated EGFR endocytosis (17). Indeed p38 kinase is not required for EGF-stimulated EGFR internalization but is required subsequently for CBL-mediated ubiquitination and degradation of internalized EGFR (21). We speculate that the phosphorylations at positions Ser^{991} and Tyr^{998} that accompany EGFR activation by ligand are normally involved in dampening the levels of phosphorylation at Ser^{1039} and Thr^{1041} as part of a mechanism to prevent receptor recycling and promote receptor destruction. In this model, the endocytosis defects associated with the S991A and Y998F variants may be due in part to inappropriate phosphorylation at Ser^{1039} and consequently uncoordinated trafficking of internalized receptors.

In conclusion, our results identify the Ser^{991} and Tyr^{998} phosphorylation sites as important determinants in ligand-stimulated EGFR endocytosis linked to p38 MAP kinase-dependent receptor phosphorylation at Ser^{1039} and Thr^{1041}. A better understanding of the mechanism by which these receptor phosphorylations are regulated and coordinated may reveal further insight into the molecular mechanisms that govern receptor recycling and degradation, which are important determinants in EGFR-directed cancer therapeutics (3, 51).

Acknowledgment—We thank Jonathan St-Germain for comments on the manuscript.

* This work was supported by funding from the Canadian Cancer Society Research Institute, Canadian Institutes of Health Research, Canada Research Chairs Program, and The McLaughlin Centre for Molecular Medicine (to M. F. M.).

S The on-line version of this article (available at http://www.mcponline.org) contains supplemental material.

‖ To whom correspondence should be addressed: The Hospital For Sick Children, MaRS East Tower 9-804, 101 College St., Toronto, Ontario M5G 1L7, Canada. Tel.: 647-235-6435; E-mail: m.moran@utoronto.ca.

REFERENCES

1. Schlessinger, J. (2002) Ligand-induced, receptor-mediated dimerization and activation of EGF receptor. *Cell* **110,** 669–672
2. Zhang, X., Gureasko, J., Shen, K., Cole, P. A., and Kuriyan, J. (2006) An allosteric mechanism for activation of the kinase domain of epidermal growth factor receptor. *Cell* **125,** 1137–1149
3. Yarden, Y. (2001) The EGFR family and its ligands in human cancer. Signalling mechanisms and therapeutic opportunities. *Eur. J. Cancer* **37,** Suppl. 4, S3–S8
4. Jones, R. B., Gordus, A., Krall, J. A., and MacBeath, G. (2006) A quantitative protein interaction network for the ErbB receptors using protein microarrays. *Nature* **439,** 168–174
5. Schulze, W. X., Deng, L., and Mann, M. (2005) Phosphotyrosine interactome of the ErbB receptor kinase family. *Mol. Syst. Biol.* **1,** 2005.0008
6. Blagoev, B., Ong, S. E., Kratchmarova, I., and Mann, M. (2004) Temporal analysis of phosphotyrosine-dependent signaling networks by quantitative proteomics. *Nat. Biotechnol.* **22,** 1139–1145
7. Zhang, Y., Wolf-Yadlin, A., Ross, P. L., Pappin, D. J., Rush, J., Lauffenburger, D. A., and White, F. M. (2005) Time-resolved mass spectrometry of tyrosine phosphorylation sites in the epidermal growth factor receptor signaling network reveals dynamic modules. *Mol. Cell. Proteomics* **4,** 1240–1250
8. Wolf-Yadlin, A., Hautaniemi, S., Lauffenburger, D. A., and White, F. M. (2007) Multiple reaction monitoring for robust quantitative proteomic analysis of cellular signaling networks. *Proc. Natl. Acad. Sci. U.S.A.* **104,** 5860–5865
9. Dengjel, J., Akimov, V., Olsen, J. V., Bunkenborg, J., Mann, M., Blagoev, B., and Andersen, J. S. (2007) Quantitative proteomic assessment of very early cellular signaling events. *Nat. Biotechnol.* **25,** 566–568
10. Olsen, J. V., Blagoev, B., Gnad, F., Macek, B., Kumar, C., Mortensen, P., and Mann, M. (2006) Global, in vivo, and site-specific phosphorylation dynamics in signaling networks. *Cell* **127,** 635–648
11. Wu, S. L., Kim, J., Bandle, R. W., Liotta, L., Petricoin, E., and Karger, B. L. (2006) Dynamic profiling of the post-translational modifications and interaction partners of epidermal growth factor receptor signaling after stimulation by epidermal growth factor using Extended Range Proteomic Analysis (ERPA). *Mol. Cell. Proteomics* **5,** 1610–1627
12. Stover, D., Caldwell, J., Marto, J., Root, K., Mestan, J., Stumm, M., Ornatsky, O., Orsi, C., Radosevic, N., Liao, L., Fabbro, D., and Moran, M. F. (2004) Differential phosphoprofiles of EGF and EGFR kinase inhibitor-treated human tumor cells and mouse xenografts. *Clin. Proteomics* **1,** 69–80
13. Heisermann, G. J., and Gill, G. N. (1988) Epidermal growth factor receptor threonine and serine residues phosphorylated in vivo. *J. Biol. Chem.* **263,** 13152–13158
14. Boeri Erba, E., Matthiesen, R., Bunkenborg, J., Schulze, W. X., Di Stefano, P., Cabodi, S., Tarone, G., Defilippi, P., and Jensen, O. N. (2007) Quantitation of multisite EGF receptor phosphorylation using mass spectrometry and a novel normalization approach. *J. Proteome Res.* **6,** 2768–2785
15. Thelemann, A., Petti, F., Griffin, G., Iwata, K., Hunt, T., Settinari, T., Fenyo, D., Gibson, N., and Haley, J. D. (2005) Phosphotyrosine signaling net-

works in epidermal growth factor receptor overexpressing squamous carcinoma cells. *Mol. Cell. Proteomics* **4,** 356–376
16. Sorkin, A., Mazzotti, M., Sorkina, T., Scotto, L., and Beguinot, L. (1996) Epidermal growth factor receptor interaction with clathrin adaptors is mediated by the Tyr974-containing internalization motif. *J. Biol. Chem.* **271,** 13377–13384
17. Zwang, Y., and Yarden, Y. (2006) p38 MAP kinase mediates stress-induced internalization of EGFR: implications for cancer chemotherapy. *EMBO J.* **25,** 4195–4206
18. Wang, Q., Zhu, F., and Wang, Z. (2007) Identification of EGF receptor C-terminal sequences 1005–1017 and di-leucine motif 1010LL1011 as essential in EGF receptor endocytosis. *Exp. Cell Res.* **313,** 3349–3363
19. Huang, F., Kirkpatrick, D., Jiang, X., Gygi, S., and Sorkin, A. (2006) Differential regulation of EGF receptor internalization and degradation by multiubiquitination within the kinase domain. *Mol. Cell* **21,** 737–748
20. Singhirunnusorn, P., Ueno, Y., Matsuo, M., Suzuki, S., Saiki, I., and Sakurai, H. (2007) Transient suppression of ligand-mediated activation of epidermal growth factor receptor by tumor necrosis factor-alpha through the TAK1-p38 signaling pathway. *J. Biol. Chem.* **282,** 12698–12706
21. Frey, M. R., Dise, R. S., Edelblum, K. L., and Polk, D. B. (2006) p38 kinase regulates epidermal growth factor receptor downregulation and cellular migration. *EMBO J.* **25,** 5683–5692
22. Tong, J., Taylor, P., Jovceva, E., St-Germain, J. R., Jin, L. L., Nikolic, A., Gu, X., Li, Z. H., Trudel, S., and Moran, M. F. (2008) Tandem immunoprecipitation of phosphotyrosine-mass spectrometry (TIPY-MS) indicates C19orf10 becomes tyrosine phosphorylated and associated with activated epidermal growth factor receptor. *J. Proteome Res.* **7,** 1067–1077
23. Davies, S. P., Reddy, H., Caivano, M., and Cohen, P. (2000) Specificity and mechanism of action of some commonly used protein kinase inhibitors. *Biochem. J.* **351,** 95–105
24. Wang, Z., and Moran, M. F. (1996) Requirement for the adapter protein GRB2 in EGF receptor endocytosis. *Science* **272,** 1935–1939
25. Zhang, L., Gjoerup, O., and Roberts, T. M. (2004) The serine/threonine kinase cyclin G-associated kinase regulates epidermal growth factor receptor signaling. *Proc. Natl. Acad. Sci. U.S.A.* **101,** 10296–10301
26. Wang, Q., Villeneuve, G., and Wang, Z. (2005) Control of epidermal growth factor receptor endocytosis by receptor dimerization, rather than receptor kinase activation. *EMBO Rep.* **6,** 942–948
27. Keller, A., Nesvizhskii, A. I., Kolker, E., and Aebersold, R. (2002) Empirical statistical model to estimate the accuracy of peptide identifications made by MS/MS and database search. *Anal. Chem.* **74,** 5383–5392
28. Nesvizhskii, A. I., Keller, A., Kolker, E., and Aebersold, R. (2003) A statistical model for identifying proteins by tandem mass spectrometry. *Anal. Chem.* **75,** 4646–4658
29. Florens, L., Carozza, M. J., Swanson, S. K., Fournier, M., Coleman, M. K., Workman, J. L., and Washburn, M. P. (2006) Analyzing chromatin remodeling complexes using shotgun proteomics and normalized spectral abundance factors. *Methods* **40,** 303–311
30. Paoletti, A. C., Parmely, T. J., Tomomori-Sato, C., Sato, S., Zhu, D., Conaway, R. C., Conaway, J. W., Florens, L., and Washburn, M. P. (2006) Quantitative proteomic analysis of distinct mammalian Mediator complexes using normalized spectral abundance factors. *Proc. Natl. Acad. Sci. U.S.A.* **103,** 18928–18933
31. Keshishian, H., Addona, T., Burgess, M., Kuhn, E., and Carr, S. A. (2007) Quantitative, multiplexed assays for low abundance proteins in plasma by targeted mass spectrometry and stable isotope dilution. *Mol. Cell. Proteomics* **6,** 2212–2229
32. Cox, D. M., Zhong, F., Du, M., Duchoslav, E., Sakuma, T., and McDermott, J. C. (2005) Multiple reaction monitoring as a method for identifying protein posttranslational modifications. *J. Biomol. Tech.* **16,** 83–90
33. Unwin, R. D., Griffiths, J. R., Leverentz, M. K., Grallert, A., Hagan, I. M., and Whetton, A. D. (2005) Multiple reaction monitoring to identify sites of protein phosphorylation with high sensitivity. *Mol. Cell. Proteomics* **4,** 1134–1144
34. Zappacosta, F., Collingwood, T. S., Huddleston, M. J., and Annan, R. S. (2006) A quantitative results-driven approach to analyzing multisite protein phosphorylation: the phosphate-dependent phosphorylation profile of the transcription factor Pho4. *Mol. Cell. Proteomics* **5,** 2019–2030
35. Covey, T., Shushan, B., Bonner, R., Schroder, W., and Hucho, F. (1991) LC/MS and LC/MS/MS screening for the sites of posttranslational modifications in proteins, in *Methods in Protein Sequence Analysis* (Jornvall, H., Hoog, J., and Gustavsson, A., eds) pp. 249–256, Birkhauser Press, Basel
36. Ficarro, S. B., McCleland, M. L., Stukenberg, P. T., Burke, D. J., Ross, M. M., Shabanowitz, J., Hunt, D. F., and White, F. M. (2002) Phosphoproteome analysis by mass spectrometry and its application to Saccharomyces cerevisiae. *Nat. Biotechnol.* **20,** 301–305
37. Yates, J. R., 3rd, Eng, J. K., McCormack, A. L., and Schieltz, D. (1995) Method to correlate tandem mass spectra of modified peptides to amino acid sequences in the protein database. *Anal. Chem.* **67,** 1426–1436
38. Batzer, A. G., Rotin, D., Ureña, J. M., Skolnik, E. Y., and Schlessinger, J. (1994) Hierarchy of binding sites for Grb2 and Shc on the epidermal growth factor receptor. *Mol. Cell. Biol.* **14,** 5192–5201
39. Old, W. M., Meyer-Arendt, K., Aveline-Wolf, L., Pierce, K. G., Mendoza, A., Sevinsky, J. R., Resing, K. A., and Ahn, N. G. (2005) Comparison of label-free methods for quantifying human proteins by shotgun proteomics. *Mol. Cell. Proteomics* **4,** 1487–1502
40. Ewing, R. M., Chu, P., Elisma, F., Li, H., Taylor, P., Climie, S., McBroom-Cerajewski, L., Robinson, M. D., O'Connor, L., Li, M., Taylor, R., Dharsee, M., Ho, Y., Heilbut, A., Moore, L., Zhang, S., Ornatsky, O., Bukhman, Y. V., Ethier, M., Sheng, Y., Vasilescu, J., Abu-Farha, M., Lambert, J. P., Duewel, H. S., Stewart, I. I., Kuehl, B., Hogue, K., Colwill, K., Gladwish, K., Muskat, B., Kinach, R., Adams, S. L., Moran, M. F., Morin, G. B., Topaloglou, T., and Figeys, D. (2007) Large-scale mapping of human protein-protein interactions by mass spectrometry. *Mol. Syst. Biol.* **3,** 89
41. Owen, D. J., and Evans, P. R. (1998) A structural explanation for the recognition of tyrosine-based endocytotic signals. *Science* **282,** 1327–1332
42. Schaefer, A. W., Kamei, Y., Kamiguchi, H., Wong, E. V., Rapoport, I., Kirchhausen, T., Beach, C. M., Landreth, G., Lemmon, S. K., and Lemmon, V. (2002) L1 endocytosis is controlled by a phosphorylation-dephosphorylation cycle stimulated by outside-in signaling by L1. *J. Cell Biol.* **157,** 1223–1232
43. Duan, L., Miura, Y., Dimri, M., Majumder, B., Dodge, I. L., Reddi, A. L., Ghosh, A., Fernandes, N., Zhou, P., Mullane-Robinson, K., Rao, N., Donoghue, S., Rogers, R. A., Bowtell, D., Naramura, M., Gu, H., Band, V., and Band, H. (2003) Cbl-mediated ubiquitinylation is required for lysosomal sorting of epidermal growth factor receptor but is dispensable for endocytosis. *J. Biol. Chem.* **278,** 28950–28960
44. Huang, F., and Sorkin, A. (2005) Growth factor receptor binding protein 2-mediated recruitment of the RING domain of Cbl to the epidermal growth factor receptor is essential and sufficient to support receptor endocytosis. *Mol. Biol. Cell* **16,** 1268–1281
45. Umebayashi, K., Stenmark, H., and Yoshimori, T. (2008) Ubc4/5 and c-Cbl continue to ubiquitinate EGF receptor after internalization to facilitate polyubiquitination and degradation. *Mol. Biol. Cell* **19,** 3454–3462
46. Waterman, H., Katz, M., Rubin, C., Shtiegman, K., Lavi, S., Elson, A., Jovin, T., and Yarden, Y. (2002) A mutant EGF-receptor defective in ubiquitylation and endocytosis unveils a role for Grb2 in negative signaling. *EMBO J.* **21,** 303–313
47. Martinu, L., Santiago-Walker, A., Qi, H., and Chou, M. M. (2002) Endocytosis of epidermal growth factor receptor regulated by Grb2-mediated recruitment of the Rab5 GTPase-activating protein RN-tre. *J. Biol. Chem.* **277,** 50996–51002
48. Yamazaki, T., Zaal, K., Hailey, D., Presley, J., Lippincott-Schwartz, J., and Samelson, L. E. (2002) Role of Grb2 in EGF-stimulated EGFR internalization. *J. Cell Sci.* **115,** 1791–1802
49. Jiang, X., Huang, F., Marusyk, A., and Sorkin, A. (2003) Grb2 regulates internalization of EGF receptors through clathrin-coated pits. *Mol. Biol. Cell* **14,** 858–870
50. Lowenstein, E. J., Daly, R. J., Batzer, A. G., Li, W., Margolis, B., Lammers, R., Ullrich, A., Skolnik, E. Y., Bar-Sagi, D., and Schlessinger, J. (1992) The SH2 and SH3 domain-containing protein GRB2 links receptor tyrosine kinases to ras signaling. *Cell* **70,** 431–442
51. Grandal, M. V., and Madshus, I. H. (2008) Epidermal growth factor receptor and cancer: control of oncogenic signalling by endocytosis. *J. Cell. Mol. Med.* **12,** 1527–1534